Journal of Solid State Chemistry 181 (2008) 2279–2284

Contents lists available at ScienceDirect

Journal of Solid State Chemistry

journal homepage: www.elsevier.com/locate/jssc

Synthesis and properties of transparent luminescent nanocomposites with surface functionalized semiconductor nanocrystals

Junfang Gao [a], Yuqin Fu [b], Xiaodan Lü [a], Yaying Du [a], Changli Lü [a,*], Zhongmin Su [a]

[a] Institute of Chemistry, Northeast Normal University, Changchun 130024, PR China
[b] College of Life Sciences, Jilin Agricultural University, Changchun 130118, PR China

ARTICLE INFO

Article history:
Received 2 December 2007
Received in revised form
8 May 2008
Accepted 8 May 2008
Available online 21 May 2008

Keywords:
Aphen
CdS nanocrystals
Ligand exchange
Bulk polymerization
Ttransparent nanocomposites
Fluorescent properties

ABSTRACT

5-Amino-1,10-phenanthroline (Aphen) was used as an organic ligand to functionalize CdS nanocrystals (NCs) by a ligand-exchange process. The functional Aphen-CdS NCs have strong luminescent emission at 552 nm and good dispersibility in the polar organic monomers. The Aphen-CdS NCs were dispersed in polymeric monomers to prepare a series of transparent luminescent nanocomposites with excellent thermal stability via in-situ bulk polymerization. The fluorescent properties of the Aphen-CdS NCs were well retained in the polymer matrix. It was found that when the methacrylic acid (MAA) and glycidyl methacrylate (GMA) as the comonomers were introduced into the polymer matrix, the emission peaks of the resultant nanocomposites had a blue shift and the fluorescent intensities also increased due to the interaction between NCs and the polymer matrices. The transparent NCs/polymer nanocomposites with tunable fluorescent emission can be potentially used for the fabrication of optoelectronic devices.

1. Introduction

Nanocrystals (NCs) have become a new class of fluorescent materials that can be used for biological labeling [1,2], optoelectronic devices [3,4] and multi-color optical encoding of biomolecules [5]. The optical properties of the semiconductor NCs can be tuned not only by changing the particle size [6], but also by the surface functionalization of NCs. The recent researches have found that the conjugation of organic functional ligands or chromophores to NCs can play an important role in the tailoring of the optical and electronic properties of NCs. For example, the use of amines as the anchors can increase the fluorescence quantum yield of NCs [7]. The optical properties of CdSe/ZnS NCs can be controlled by surface coating with the calix-[*n*]arene derivatives [8]. Organic photochromic dye can be attached to NCs to reversibly modulate the fluorescence emission of NCs [9,10]. In addition, the NCs/polymer nanocomposites with functionality have attracted more attention due to their electrical, optical, magnetic, and optoelectronic properties [11–18]. However, the small size NCs with high specific surface energy and inherent hydrophilic character are prone to aggregation, so the preparation of transparent bulk nanocomposites with NCs dispersed uniformly is still a challengeable work.

Aphen is one of the widely adopted chelating ligands in coordination chemistry. The ligand and its complex have many applications in different fields, such as in molecular catalysis, solar energy conversion, molecular recognition, self-assembly, and nucleic acid probes [19–21]. In this paper, Aphen was used to decorate the CdS NCs via a ligand-exchange process. The amino group of Aphen on the CdS surface is an outer functional group, which can react or interact with the groups of polymer chains, and thus the fluorescent properties of the resulting composite NCs can be adjusted by this way. The mercaptoethanol (ME) capped CdS NCs were firstly synthesized through chemical wet method and were functionalized with Aphen via a ligand-exchange process, then the resultant composite CdS NCs (Aphen-CdS NCs) with good luminescence properties were incorporated into the polymer matrices to fabricate transparent fluorescent nanocomposites by in-situ bulk polymerization (Scheme 1). The structure, microstructure and optical properties as well as thermal stability of the functionalized NCs and their nanocomposites were studied in detail.

2. Experimental section

2.1. Materials

5-Amino-1,10-phenanthroline (Aphen) was synthesized from 1,10-phenanthroline by nitration and reduction process as

* Corresponding author. Fax: +86 43185098768.
E-mail address: lucl055@nenu.edu.cn (C. Lü).

0022-4596/$ - see front matter © 2008 Elsevier Inc. All rights reserved.
doi:10.1016/j.jssc.2008.05.024

described previously [22]. *N*,*N*-dimethylacrylamide (DMAA), styrene (St), divinylbenzene (DVB), glycidylmethacrylate (GMA), and methacrylic acid (MAA) were distilled under vacuum prior to use. 2,2′-Azobisisobutyronitrile (AIBN, 98%) was recrystallized from methanol. Cadmium acetate dihydrate ($Cd(Ac)_2 \cdot 2H_2O$), 2-mercaptoethanol (ME), thiourea and *N*,*N*-dimethylformamide (DMF) were analytical grade reagents and were used without further purification.

2.2. Synthesis of CdS NCs

CdS NCs (ME-capped CdS NCs) were synthesized from $Cd(Ac)_2 \cdot 2H_2O$ and thiourea by one-step process in DMF. $Cd(Ac)_2 \cdot 2H_2O$ (7.729 g, 0.029 mol), thiourea (1.568 g, 0.021 mol), and ME (2.812 g, 0.036 mol) were dissolved in 580 mL of DMF, then the mixture was poured into a 1000 mL three-necked round-bottom flask fitted with a magnetic stirrer, a reflux condenser and a nitrogen inlet. The reaction solution was stirred at 120 °C for 10 h, and then concentrated to 100 mL under a reduced pressure. The product was precipitated from ethanol (300 mL), and finally, 5.98 g of CdS NCs was obtained after drying at room temperature under vacuum.

2.3. Synthesis of Aphen-CdS NCs

In all, 3.0 g of CdS NCs and 0.1 g of Aphen were dissolved in 60 mL of DMF. After stirring for 30 h at room temperature, the reaction solution was poured into 500 mL of ethanol. The precipitate was washed with ethanol (100 mL) four times, and then centrifuged and dried at room temperature in vacuum. Finally, 2.82 g of Aphen-CdS NCs as yellow powder was obtained and the particles have good dispersibility in DMAA, DMF, and DMSO.

2.4. Preparation of Aphen-CdS NCs/polymer nanocomposites

The ME-capped CdS and Aphen-CdS NCs were introduced into the polymer matrix by in-situ bulk polymerization, respectively. The experimental recipes are listed in Table 1. Different weights of CdS NCs were dispersed in the mixture monomers of DMAA, St, and DVB under ultrasonic vibration. The weight ratio of DMAA:St:DVB is 27:1:2. To study the effect of monomer groups on the optical properties of the nanocomposites, methacrylic acid (MAA) and glycidyl methacrylate (GMA) were used as comonomers to introduce into the polymer matrix. In order to ensure the functional monomer is in excess with respect to the Aphen molecules on the surface of CdS NCs, the weight ratio of MAA and GMA to Aphen-CdS NCs was kept at 7.3 and 12, respectively. Subsequently, 0.4 wt% AIBN was added to the above transparent dispersion and the systems were polymerized at 60 °C for 12 h and 120 °C for 2 h. Finally, a series of transparent bulk nanocomposites were obtained by the above procedure.

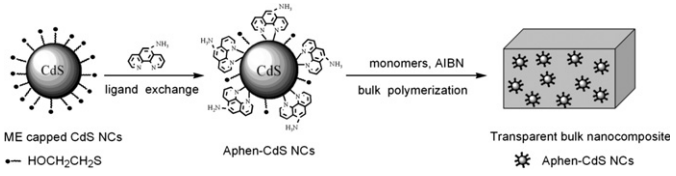

Scheme 1. Preparative scheme of the Aphen functionalized CdS NCs and their luminescent nanocomposites by ligand-exchange process and in-situ bulk polymerization.

2.5. Characterization

FTIR spectra were recorded on a Nicolet AVATAR360 FTIR spectrometer. ^{1}H-NMR spectra were obtained from an AVANCE 500 MHz Bruker spectrometer in d_6-DMSO. UV-vis absorption spectra were recorded on a Shimadzu 3100 UV-vis-NIR spectrometer in the range 200–800 nm. The photoluminescence properties of NCs were measured on a Cary Eclipse fluorescence spectrometer. Transmission electron microscopy (TEM) was carried out using a JEOL-2021 microscope. The wide-angle X-ray diffraction (WAXD) measurement was performed on a PW1710 BASED X-ray diffractometer with Cu$K\alpha$ ($\lambda = 1.5418$ Å) radiation. Thermogravimetric analysis (TGA) was performed on a Perkin-Elmer TGA7 at a heating rate of 10 °C min^{-1} under nitrogen flow from 50 to 750 °C.

3. Results and discussion

3.1. Structure and fluorescent characterization of functionalized CdS nanocrystals

Fig. 1 shows the FTIR spectra of the Aphen, CdS, and Aphen-CdS NCs. It can be seen that both of the two NCs exhibit the characteristic peaks of hydroxyl groups of ME at 3420 cm^{-1}. Compared with the CdS NCs, the absorption intensity at 1630 cm^{-1} obviously increases in the spectrum of the Aphen-CdS NCs. This peak is assigned to the characteristic absorption of $\nu_{C=C}$ in Aphen on the surface of CdS NCs, although the CdS NCs also exhibit a weak absorption at this wavenumber. The new absorption peak at 1460 cm^{-1} is also ascribed to the above $\nu_{C=C}$ vibration. The ^{1}H-NMR data also testify that Aphen has attached to the surface of CdS NCs. Fig. 2 shows the ^{1}H-NMR spectra of Aphen-CdS NCs and Aphen in d_6-DMSO. When Aphen is attached to the CdS NCs, the characteristic peaks of Aphen on the NCs surface broaden and the chemical shifts also obviously change as compared to the pure Aphen. The peaks of Aphen at $\delta = 6.13$ (2H, $-NH_2$), 6.86 (1H, 6-Aphen-H), and 7.49–7.75 (2H, 3, 8-Aphen-H)

Table 1
Recipes for the synthesis of different NCs-polymer nanocomposites and their maximum emission wavelengths

Sample	Content of NCs (wt%)[a]	Recipes					λ_{em} (nm)
		APhen-CdS (mg)	CdS (mg)	DMAA–St–DVB (g)[b]	MAA (g)	GMA (g)	
1	0	–	–	4.5	–	–	460
2	1	–	45	4.5	–	–	511
3	0.1	4.5	–	4.5	–	–	505
4	1	45	–	4.5	–	–	538
5	1	45	–	4.5	0.33	–	526
6	1	45	–	4.5	–	0.54	529

[a] The weight percent content of NCs in polymer matrix.
[b] The total weight of the three monomers (the weight ratio of the monomers is fixed as DMAA:St:DVB = 27:1:2).

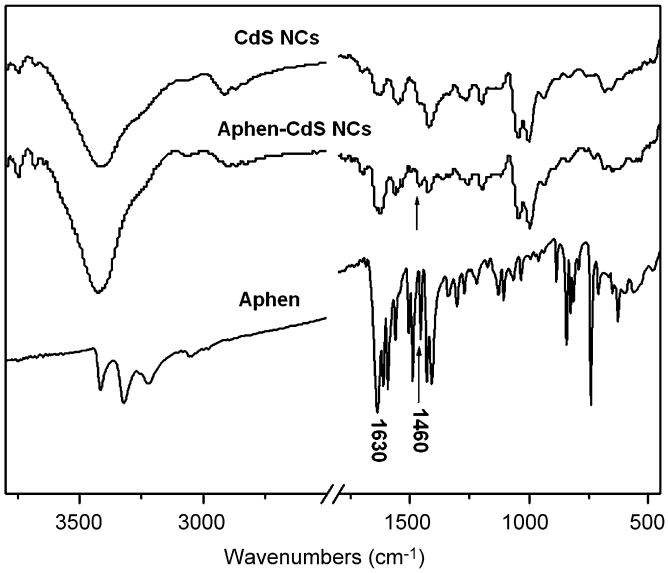

Fig. 1. FTIR spectra of Aphen, CdS, and Aphen-CdS NCs.

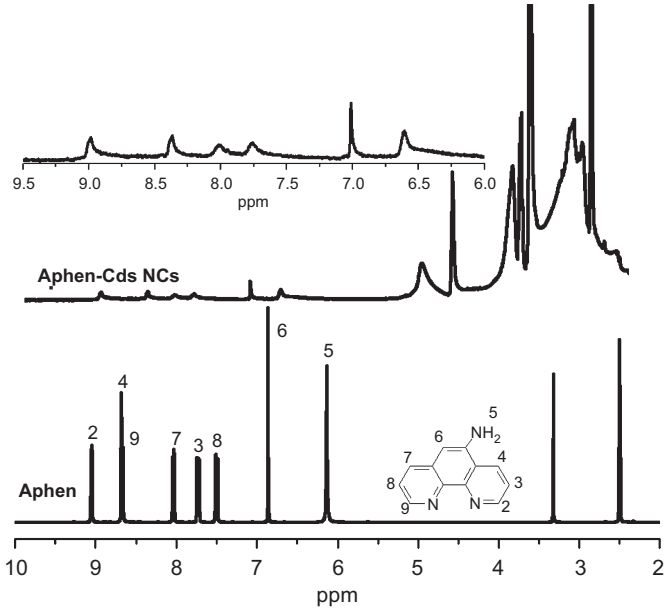

Fig. 2. ^{1}H-NMR spectra of Aphen and Aphen-CdS NCs in d_6-DMSO.

shift to low field (6.7, 7.08 and 7.77–8.01) owing to the change of the chemical circumstance. The two peaks at $\delta = 8.04$ and 8.68 (2H, 4, 7-Aphen-H) as well as another two peaks at $\delta = 8.66$ and 9.06 (2H, 2, 9-Aphen-H) combine to form two single peaks at $\delta = 8.35$ and 8.94, respectively. These results indicate that the Aphen functionalized CdS NCs have been successfully obtained by the ligand-exchange procedure.

The XRD patterns of the NCs are shown in Fig. 3. Three diffraction peaks at 26.5°, 43.6°, and 51.5° can be indexed as (111), (220), and (311) planes of cubic CdS phase [23]. According to the XRD patterns, we use Scherrer diffraction formula relating diffraction angular width (β) to the domain size (D) to calculate the diameter of CdS and Aphen-CdS NCs [24]:

$$D = k\lambda/\beta \cos\theta$$

where $k = 1$ for the CdS cubic structure, λ is the X-ray wavelength (1.541 Å), and θ the diffraction angle. From the XRD results, the

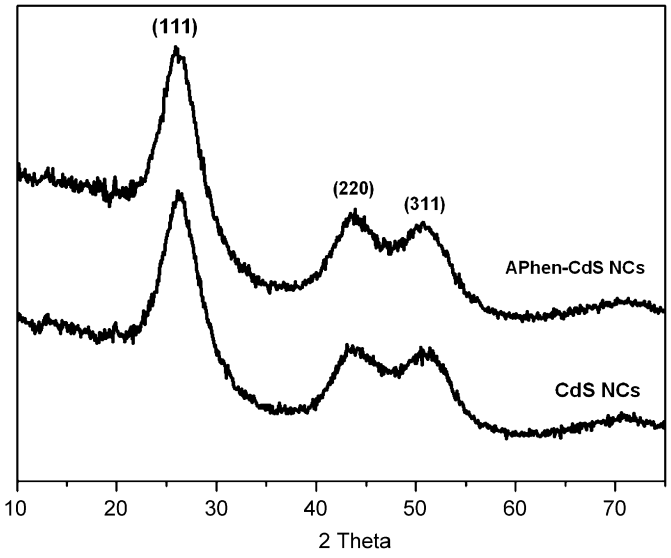

Fig. 3. X-ray diffraction patterns of CdS and Aphen-CdS NCs.

diameters of both CdS and Aphen-CdS NCs were calculated to be about 3.4 nm, indicating that the size of CdS NCs did not change after surface ligand exchange. This result is well in agreement with the TEM analysis. Fig. 4a and b shows the TEM images of CdS and Aphen-CdS NCs. It can be seen that the two NCs with a mean diameter of 3–5 nm dispersed homogeneously without aggregation, which will provide the precondition for the following integration of these NCs into transparent polymers.

The photoluminescence properties of the Aphen, CdS, and Aphen-CdS NCs were studied and their PL spectra (Fig. 5) were obtained by employing an exciting wavelength at 460 nm (the exciting wavelength of Aphen is 310 nm). It can be seen that the pure Aphen has a strong emission peak at 474 nm. The broad fluorescent emission of CdS NCs at 600 nm originates from the surface defects of NCs, while the Aphen-CdS NCs exhibit a blue shift of emission peak appeared at 552 nm after the ligand exchange as compared with CdS NCs, indicating that Aphen has attached to the CdS NCs surface and formed the composite NCs. It is known that the complex of phenanthroline or its derivatives with metal ions also has the fluorescent emission character, and thus it is possible that the coordination effect of the organic fluorophores with the cadmium atom on the surface of semiconductor NCs results in the interesting luminescent properties for Aphen-CdS NCs, and this fluorescent emission may have a cooperating effect with the inherent emission of CdS NCs. However, it still needs more effort to clarify the detailed mechanism.

3.2. Photoluminescence, microstructure, and thermal properties of transparent nanocomposites

It is known that the polymer as a soft matter is an alternative matrix for the composite of inorganic nanoparticles to carry out their function and processability. Here, we have integrated the functionalized NCs into the polymer matrix to prepare a series of transparent fluorescent nanocomposites via in-situ bulk polymerization. We selected the DMAA, St, and DVB as the comonomers to obtain the polymer matrix for the composite of NCs. For the Aphen-CdS NCs, it should be noted that the amine group of Aphen on the surface of NCs can react or form hydrogen bond with other groups such as carboxyl or epoxy groups in polymer, and thus the emission properties will be affected. So here, the MAA and GMA were also used as comonomers to study the effect of polymer

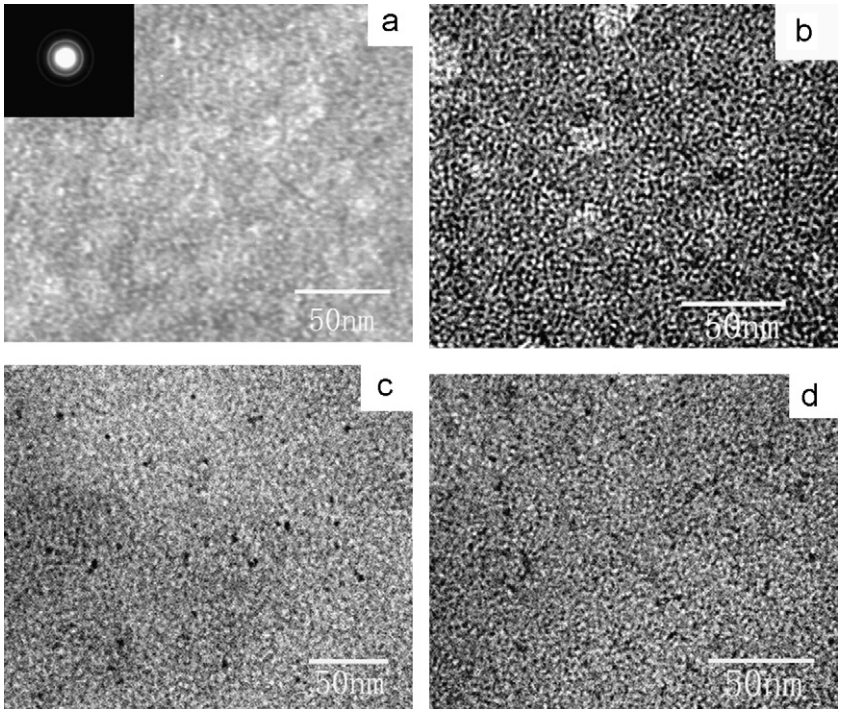

Fig. 4. TEM images of CdS NCs (a), Aphen-CdS NCs (b), nanocomposite samples 4(c) and 5(d).

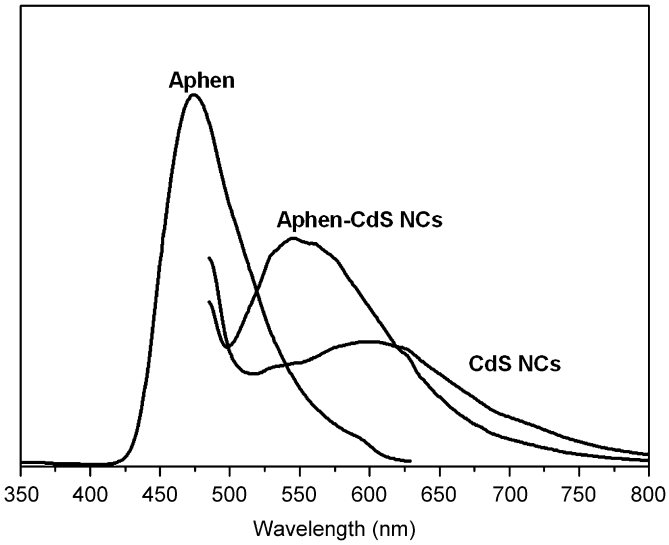

Fig. 5. Fluorescent emission spectra of Aphen, Aphen-CdS, and CdS NCs.

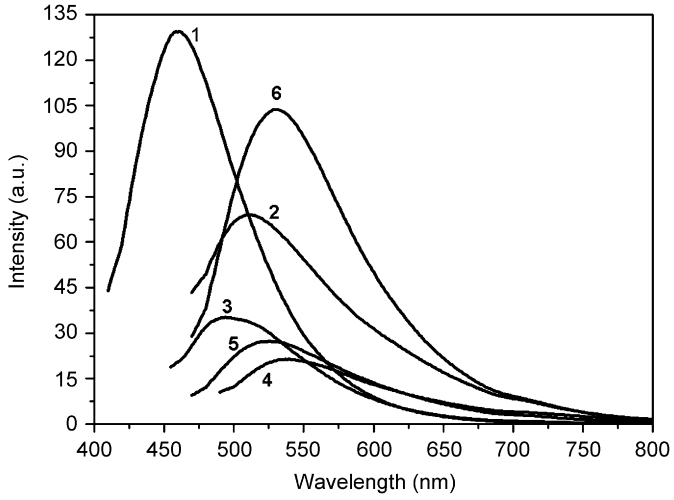

Fig. 6. Fluorescent emission spectra of different nanocomposite samples. The numbers of the nanocomposite samples are responding to that in Table 1.

environment on the fluorescent emission of NCs, because the polymer containing MAA or GMA units may induce the change of the fluorescent properties of Aphen-CdS NCs.

Fig. 6 shows the PL spectra of polymer matrix and different NCs/polymer nanocomposites. The sample numbers in Fig. 6 are consistent with that listed in Table 1. It should be noted that the pure polymer matrix obtained from DMAA–St–DVB exhibits a blue emission at 460 nm probably originated from the contribution of PDMAA segments [25]. When Aphen-CdS NCs are introduced in the polymer, the nanocomposites exhibit a complicated photoluminescence property with the content change of NCs in polymer (see Fig. 6). The fluorescent emission peaks of the nanocomposites exhibit a blue shift (460–538 nm) as compared with that of Aphen-CdS NCs, while their fluorescence intensities decrease with increasing NCs concentration from 0.1 to 1 wt%. We consider that the interaction between Aphen-CdS NCs and PDMAA segments in the polymer matrix may result in the shift of the emission peak and partial fluorescent quenching of nanocomposites. From the PL spectra of the obtained NCs/polymer nanocomposites with the same NCs concentration (Fig. 6), it also can be seen that as the CdS and Aphen-CdS NCs were introduced into polymers, the maximum emission peaks (511–538 nm) of all the nanocomposite samples have a blue shift as compared with that of their NCs (the maximum emission peaks of CdS and Aphen-CdS NCs are 600 and 552 nm, respectively). Especially, the CdS NCs/polymer (sample 2) nanocomposite exhibits a maximum blue shift of about 90 nm and higher emission intensity when compared to sample 4, although the Aphen-CdS NCs have stronger emission than CdS NCs. This phenomenon may be attributed to the interaction between NCs and the polymer matrix, which

affects the surface state emission of NCs. Because the Aphen molecules have a large molecule volume and rigidity, Aphen-CdS NCs have bigger surface steric hindrance than the CdS NCs as the polymer containing PDMAA segments interacts with the NCs. As a result, the surface defects of CdS NCs can be more effectively improved, which results in the maximum blue shift and increasing intensity of fluorescent emission of CdS NCs in sample 2. In addition, the decrease of the emission intensity for the Aphen-CdS/polymer (sample 4) than sample 2 may be the result of the fluorescent quenching of organic chromophore decorated NCs in the polymer matrix. However, when the GMA and MAA with reactive groups (epoxy or carboxyl groups) were introduced in the polymer matrix, it is interesting that samples 5 and 6 exhibit the further blue shift and increasing fluorescent intensity as compared with sample 4. Especially, sample 6 with GMA segments exhibits the stronger fluorescent emission, even than sample 2. This result may be due to the interaction of covalent bonds or hydrogen bonds formed by carboxyl groups of MAA or epoxy groups of GMA with amino groups on the surface of Aphen-CdS NCs, which decreases the fluorescent concentration quenching of the organic chromophore on NCs and improves the fluorescence emission of the composite NCs with the organic chromophore. However, now we have difficulty to provide the direct evidence for the interaction of Aphen on surface of NCs with the MAA or GMA segments in the polymer because the content of Aphen on NCs in the polymer matrix is very low. To clarify the effect of the comonomer (MAA or GMA) concentration on the fluorescence properties of composites, we also changed the comonomer contents in samples 5 and 6 by decreasing the addition amount of MAA or GMA in the polymer to 0.033 and 0.054 g. We found that the variation of the comonomer concentrations did not evidently affect the fluorescence emission of the resulted nanocomposite samples. In addition, as the MAA and GMA comonomers were introduced into sample 2 with CdS NCs, the PL spectra of the nanocomposites still did not obviously change when compared with that of sample 2. This result further proves that the interaction between $-NH_2$ in Aphen on Aphen-CdS NCs and the MAA or GMA segments in the polymers resulted in the change of photoluminescent properties of the NCs/polymer nanocomposites. Fig. 7 shows the PL photographs of the different nanocomposites excited by an UV light at 365 nm. These nanocomposites present strong PL emission and their emission colors are consistent with their PL spectra.

All the fluorescent nanocomposites possess excellent optical transparency and there no macroscopic phase separation was observed. TEM analyses also supported this result. Fig. 4c and d is the TEM images of samples 4 and 5. It can be seen that the Aphen-CdS NCs are well dispersed in the polymer matrices. The size and morphology of Aphen-CdS NCs are similar to that before incorporation into polymers without any aggregation. This result indicates that our method permits functional NCs to possess well

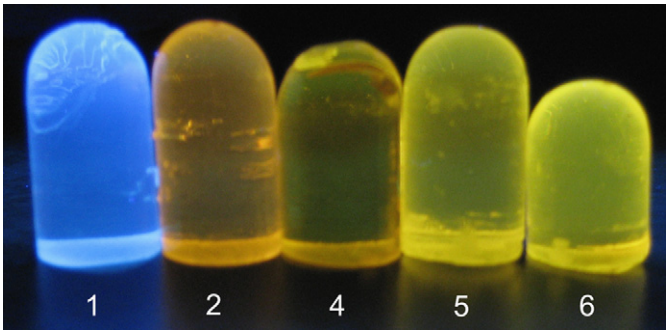

Fig. 7. PL photographs of the nanocomposites exposed under a UV lamp of 365 nm.

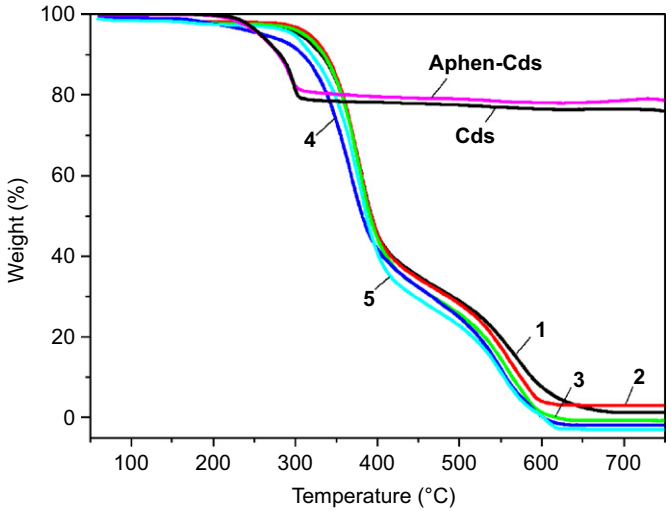

Fig. 8. TGA curves of CdS NCs, Aphen-CdS NCs, and different nanocomposite samples.

dispersibility in the transparent bulk polymer matrices, which is very important for the photoluminescence properties of the resultant nanocomposites. Here, the monomer DMAA as the primary comonomer plays a key factor for preparing the transparent bulk nanocomposites [26].

Fig. 8 presents the TGA curves of the CdS NCs, Aphen-CdS NCs, and nanocomposite samples. The CdS NCs and Aphen-CdS NCs exhibit a similar loss weigh profile and they begin to decompose at above 210 °C because of the unstable ME on their surfaces. The final residues of NCs at 750 °C are 76 and 78 wt% which corresponds to the pure CdS content in the capped NCs, respectively. It can be seen that there are a large number of surface capping agents of ME (about 20 wt%) and a small quantity of Aphen on the surface of NCs. The ME molecules on the NCs help to their uniform dispersion in the polymer matrix. As the CdS and Aphen-CdS NCs are incorporated into the polymer matrix to form the bulk nanocomposites by in-situ bulk polymerization, the resulting nanocomposites have a similar thermal stability as the polymer matrix. The bulk nanocomposites show an obvious weight loss between 210 and 310 °C, which is similar to that observed in Aphen-CdS NCs. The TGA results indicate that the obtained transparent fluorescent bulk nanocomposites possess well thermal stability for the practical application.

4. Conclusions

We had synthesized the Aphen functionalized CdS NCs with strong fluorescent emission and well dispersibility via a ligand-exchange process, and the obtained NCs were also incorporated into the transparent polymer matrix to fabricate the fluorescent nanocomposites by in-situ bulk polymerization. The photoluminescence of the nanocomposites had obvious blue shift due to the effect of polymer medium as compared with the corresponding NCs within them. When the monomers MAA and GMA with functional groups were used as comonomers, the fluorescent properties of the resultant nanocomposites can be further tuned by the interaction of the covalent bonds or hydrogen bonds between functional groups in polymers and amino groups on the surface of Aphen-CdS NCs. Our strategy provided a facile process for the surface functionalization of NCs and their integration into transparent bulk polymers. The obtained functional NCs and their fluorescent nanocomposites can be potentially used in the

fabrication of multifunctional optoelectronic devices or optical materials.

Acknowledgments

This work was supported by the Training Fund of NENU'S Scientific Innovation Project (NENU-STC07003) and Analysis and Testing Foundation of Northeast Normal University.

References

[1] M.J. Bruchez, M. Moronne, P. Gin, S. Weiss, A.P. Alivisatos, Science 281 (1998) 2013.
[2] W.C.W. Chan, S. Nie, Science 281 (1998) 2016.
[3] S. Coe, W.K. Woo, M. Bawendi, V. Bulovic, Nature 420 (2002) 800.
[4] J.S. Steckel, J.P. Zimmer, S. Coe-Sullivan, N.E. Stott, V. Buloviæ, M.G. Bawendi, Angew. Chem. Int. Ed. 43 (2004) 2154.
[5] M. Han, X. Gao, J.Z. Su, S. Nie, Nat. Biotechnol. 19 (2001) 631.
[6] B.O. Dabbousi, J. Rodriguez-Viejo, F.V. Mikulec, J.R. Heine, H. Mattoussi, R. Ober, K.F. Jensen, M.G. Bawendi, J. Phys. Chem. B 101 (1997) 9463.
[7] D.V. Talapin, A.L. Rogach, A. Kornowski, M. Haase, H. Weller, Nano Lett. 1 (2001) 207.
[8] T. Jin, F. Fujii, E. Yamada, Y. Nodasaka, M. Kinjo, J. Am. Chem. Soc. 128 (2006) 9288.
[9] I.L. Medintz, S.A. Trammell, H. Mattoussi, J.M. Mauro, J. Am. Chem. Soc. 126 (2004) 30.
[10] L.Y. Zhu, M.Q. Zhu, J.K. Hurst, A.D.Q. Li, J. Am. Chem. Soc. 127 (2005) 8968.
[11] L.L. Beecroft, C.K. Ober, Chem. Mater. 9 (1997) 1302.
[12] W. Caseri, Macromol. Rapid Commun. 21 (2000) 705.
[13] H. Zhang, Z.C. Cui, Y. Wang, K. Zhang, X.L. Ji, C.L. Lü, B. Yang, M.Y. Gao, Adv. Mater. 15 (2003) 777.
[14] M.G. Kanatzidis, C.G. Wu, H.O. Marcy, M.C.R. Kannewurf, J. Am. Chem. Soc. 111 (1989) 4139.
[15] A.P. Alivisatos, J. Phys. Chem. 100 (1996) 13226.
[16] M. Takafuji, S. Ide, H. Ihara, Z. Xu, Chem. Mater. 16 (2004) 1977.
[17] E. Müh, H. Frey, J.E. Klee, R. Mülhaupt, Adv. Funct. Mater. 11 (2001) 425.
[18] C. Woelfle, R.O. Claus, Nanotechnology 18 (2007) 025402.
[19] Y. Shen, B.P. Sullivan, Inorg. Chem. 34 (1995) 6235.
[20] Z. Murtaza, P. Herman, J.R. Lakowicz, Biophys. Chem. 80 (1999) 143.
[21] D. Roberto, R. Ugo, F. Tessore, E. Lucenti, S. Quici, S. Vezza, P. Fantucci, I. Invernizzi, S. Bruni, I. Ledoux-Rak, J. Zyss, Organometallics 21 (2002) 161.
[22] K. Binnemans, P. Lenaerts, K. Driesen, C. Görller-Walrand, J. Mater. Chem. 14 (2004) 191.
[23] N.V. Smith, X-ray Powder Data Files, American Society for Testing and Materials, Philadelphia, 1967.
[24] A. Guinier, X-ray Diffraction, Freeman, San Francisco, CA, 1963.
[25] B. Yan, D. Chen, X. Jiao, Mater. Res. Bull. 39 (2004) 1655.
[26] C. Lü, Y. Cheng, Y. Liu, F. Liu, B. Yang, Adv. Mater. 18 (2006) 1188.